

THE ROLE OF REACTIVE ELEMENTS IN THERMAL BARRIER COATINGS

With the assistance of high-performance computing, the authors employ density functional theory (DFT) calculations to investigate atomic-level interactions at interfaces between ceramics and metals. They present their findings, based on DFT calculations, characterizing ideal interfaces related to those present in typical thermal barrier coatings.

The thermal barrier coating (TBC) of jet engine turbines permits operation at what otherwise would be prohibitively high temperatures. Ideally, a jet engine should operate at very high temperatures to maximize fuel efficiency and power. Combustion gases are often held at temperatures above 1370° C, while engine metal superalloys have melting points that range between 1230° and 1315° C. As a result, engine turbine blades must be cooled by flowing air through holes drilled in the blade or be protected from the hot combustion gases by some form of thermal barrier. Cooling results in a rather minimal gain in allowable combustion gas inlet temperature; such a technique's effectiveness is counterbalanced by a decrease in engine efficiency. Therefore, it is important to develop a ceramic coating to act as a thermal barrier that increases the operational lifetime of jet engines and permits higher operating temperatures, thereby increasing thrust and fuel efficiency.¹ The TBC of choice, a thin yttria-stabilized-zirconia (YSZ) coating, reduces the temperature to which the

underlying superalloy is exposed by hundreds of degrees Celsius.

A TBC consists of three primary layers that cover the macroscopic engine superalloy: the YSZ thermal protective layer, the thermally grown oxide (TGO) formed through bond coat oxidation, and the metal alloy bond coat composed of Ni (Co) CrAlY. Figure 1 shows a schematic representation of a TBC's cross section.

Our interface studies provide insight into atomic-level culprits in observed TBC failure in the form of *spallation*, a process where the TBC peels off the underlying substrate. Improving the bond coat performance might provide the most fruitful avenue for limiting TBC spallation. Accordingly, we explore the effect of chemical modifications to the bond coat alloy on ceramic/metal interface adhesion and discuss implications for macroscopic systems based on our atomic-level DFT calculations.

Spallation and oxidation

Unfortunately, a TBC's operational lifetime is limited by spallation. To help minimize spallation, a bond coat alloy is deposited on the superalloy substrate before the YSZ topcoat is applied. The bond coat's non-nickel elements are chosen to promote adhesion and improve the thermal expansion matching between the top-

Reactive Elements in TBCs

For years, reactive elements have been added to the bond coat used in TBCs. Some of the unfavorable properties associated with the alumina protective scale may be alleviated by adding specific reactive elements or using novel processing techniques. Obviously, some metal alloy oxidation and corrosion will take place. Assuming a layer of metal oxide is formed, several key factors might be explored for improved scale adhesion. In their review of studies that explored some chemical means of improving oxidation resistance of high-temperature alloys, D.P. Whittle and J. Stringer identified six mechanisms that might explain the improved oxidation resistance achieved with reactive element additions: enhanced oxide-scale plasticity, a graded seal mechanism, modification of the oxide's growth process, chemical bonding, a vacancy sink model, and "pegging" by other oxides.¹ Our atomic-level calculations relate to *chemical bonding*, although they could apply to other aspects as well.

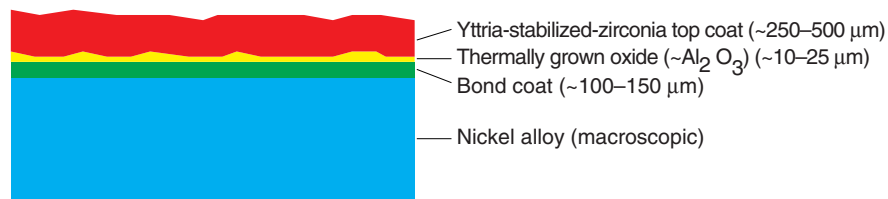
Dispersions of other oxides in the protective scale might be helpful but are generally of neutral consequence in alumina scales. Conversely, the secondary oxide inclusions (including tantalum, zirconium, and hafnium) that form at the oxide/alloy interface can effectively serve as pegs (oxide "fingers" that grow from the alloy region into the alumina (TGO) layer) to dramatically limit spallation.² Smooth regions at the interface are much more likely to de-adhere than regions where these oxide pegs are formed across the interface.

Some researchers have observed oxidation rate reduction of metal alloys through reactive element addition; early transition metals such as scandium and yttrium might serve this role.³ However, conflicting evidence exists suggesting

that, for instance, yttrium might have either no effect or even a harmful effect on weight gain (oxidation) compared to the undoped alloy.⁴ Some evidence suggests that silicon might be a promising nonmetal for limiting alloy oxidation.

Titanium is one reactive element of interest. Although it is included in some turbine superalloys, it is essentially nonexistent in state-of-the-art superalloy content. In Al_2O_3 , Ti^{4+} is thought to create cation vacancies and increase the oxide creep rate. In spite of this, it seems that oxide plasticity does not improve. In a nickel alloy, titanium can form cubic γ' precipitates, which can in turn serve as strengthening elements similar to Ni_3Al in the superalloy. Whereas certain intermetallics had been considered unfavorable due to brittleness and low temperature fracture, recent improved processing techniques for the intermetallics Ti_3Al , TiAl , Ni_3Al , and so on has helped create stronger and more ductile alloys. Likewise, titanium (and silicon) additions to bond coating alloys can improve the coefficient of thermal expansion desired for such alloys. TiAl -based intermetallics show improved hot corrosion resistance relative to nickel superalloys and might form adherent alumina (or alumina and titania scales) and limit sulfur content at the interface.⁵ Furthermore, it is possible to create interfaces exhibiting good adhesion between nickel and TiAl . Oxidation-induced embrittlement of titanium alloys has limited their application despite their intrinsic high specific strengths, but alloying with aluminum and forming an alumina protective oxide can limit or even prevent embrittlement. Such embrittlement might not pose difficulties in all TBC applications because the problems associated with titanium oxidation, which have contributed to its lack of use in bond coat alloys, should not be as significant in alumina-forming alloys compared to older alloys that formed chromia protective oxides. Although pure TiO_2 is

Figure 1.
Cross section
of a thermal
barrier
coating.



coat and substrate by providing an intermediate thermal expansion between these layers. As a result of the YSZ topcoat's transparency to high-temperature oxygen diffusion, the non-nickel elements must also serve the crucial role of protecting nickel from hot oxidation and corrosion. This protection is achieved by forming an adherent protective scale, primarily alumina for nickel alloy applications. Although chromia is a popular protective scale, it presents several drawbacks: for instance, it tends to evaporate in the

form of CrO_3 (g) above 1000°C and is not as widely used for protective scale applications as it once was. Alumina provides a more ideal scale but can exhibit poorer adhesion to the substrate compared to chromia. In addition to poor adhesion, the thermal expansion coefficient of alumina is lower than the zirconia topcoat, so thick layers cause additional strain. Nevertheless, because of its favorable properties as a protective, slow-growing oxide, alumina is the protective TGO of choice for TBC applications.

not expected to exhibit high oxidation resistance, TiO₂ dispersions in alumina do not lead to poor oxidation resistance, presumably dominated by Al₂O₃'s behavior.⁶ Accordingly, although conflicting data exists regarding how helpful or harmful titanium additions might be in complex systems, titanium's potentially helpful properties make it an element of interest.

In addition to oxidative corrosion, sulfur is expected to induce de-adhesion and spallation when present at the alloy/oxide interface. Reactive element additions of yttrium, lanthanum, cerium, and platinum might also be important in limiting sulfur's interfacial segregation. Yttrium, lanthanum, and cerium can form X₂O₂S compounds, which could explain their effectiveness in reducing sulfur diffusion. The role of platinum is not clearly understood. Although platinum is helpful in scale adhesion, a study by Bruce Pint and his colleagues found that it was not as effective in promoting scale adhesion as zirconium and hafnium.⁷ Although platinum–aluminide coatings have become popular bond coating materials recently, this finding and the poor resistance of this coating to low-temperature hot corrosion⁸ motivate continued investigation.

Although Whittle and Stringer's review stressed that the crucial aspect of reactive element addition is that the added element have a higher affinity for oxygen than the element desired to form the protective scale,¹ results of subsequent studies discussed here do not seem to follow such a simple trend.^{2–7} Although platinum has a weak affinity for oxygen, it might be a helpful addition. Likewise, ΔH_f° values for silicon, titanium, and zirconium oxides are less negative than aluminum; ΔH_f° values for hafnium, lanthanum, and cerium oxides are similar to aluminum; and the ΔH_f° 's for scandium and yttrium oxides are more negative than aluminum per mole of oxygen. Because el-

ements in each of those categories seem to be helpful reactive elements, a general rule of thumb based on oxygen affinity is overly simplistic.

References

1. D.P. Whittle and J. Stringer, "Improvements in High Temperature Oxidation Resistance by Additions of Reactive Elements or Oxide Dispersions," *Philosophical Trans. Royal Society of London*, vol. 295, no. 1413, 1980, pp. 309–329.
2. C. Mennicke et al., "The Role of Secondary Oxide Inclusions ("Pegs") on the Spalling Resistance of Oxide Films," *Acta Materialia*, vol. 48, no. 11, June 2000, pp. 2941–2949.
3. I.M. Allam, D.P. Whittle, and J. Stringer, "The Oxidation Behavior of CoCrAl Systems Containing Active Element Additions," *Oxidation of Metals*, vol. 12, no.1, Feb. 1978, pp. 35–66.
4. J.D. Kuenzly and D.L. Douglas, "The Oxidation Mechanism of Ni₃Al Containing Yttrium," *Oxidation of Metals*, vol. 8, no.3, 1974, pp.139–178.
5. Z. Tang, F. Wang, and W. Wu, "Hot Corrosion Behavior of TiAl-based Intermetallics in Molten Salts," *Oxidation of Metals*, vol. 51, nos. 3–4, Apr. 1999, pp. 235–250.
6. G. Chen and H. Lou, "Oxidation Behavior of Sputtered Ni-Cr-Al-Ti Nanocrystalline Coating," *Surface and Coatings Technology*, vol. 123, no. 1, Jan. 2000, pp. 92–96.
7. B.A. Pint et al., "Substrate and Bond Coat Compositions: Factors Affecting Alumina Scale Adhesion," *Materials Science and Eng.*, vol. 245, no. 2, May 1998, pp. 201–211.
8. G.W. Goward, "Progress in Coatings for Gas Turbine Airfoils," *Surface and Coatings Technology*, vols. 108–109, nos. 1–3, Oct. 1998, pp. 73–79.

Silica also might provide a useful protective scale due to its slow growth rate, oxidation resistance, and strength at high temperatures. The addition of silicon to certain bond coat alloys might reduce oxidation significantly and possibly improve protective scale performance.² Unfortunately, alloys with high aluminum and silicon content might also exhibit excessive interdiffusion with the underlying alloy and be quite susceptible to corrosion with certain combustion gas compositions.³ Nevertheless, SiO₂ shows some promise in high-temperature applications, and further exploration could prove useful.

A survey of reactive element additions provides some clues regarding possible helpful elements, but different experiments are difficult to compare with one another (see the sidebar). The results are not always reproducible due to uncontrolled defects and discrepancies in measur-

ing techniques. Therefore, a strong incentive for employing theoretical techniques to determine optimal reactive element additions to the bond coat exists. Due to computational size constraints, we are limited in the system complexity we can address; but, we can systematically modify the chemical composition and isolate several aspects of interfacial bonding—an impossible task from an experimental standpoint.

Computational methods

With the advent of HPC, we can use first principles DFT calculations to investigate atomic-level interactions at ideal interfaces related to TBC applications. Although the system is limited to at most a few hundred atoms due to computational size constraints, the 3D periodic boundary conditions simulate an effectively "infinite" in-

interface, neglecting long-ranged relaxation effects.

We perform spin-polarized DFT calculations using the Vienna Ab Initio Simulation Package (VASP).⁴ These calculations expand the valence electron density in a plane-wave basis and replace the core electrons with ultrasoft pseudopotentials. Nonlinear partial core corrections to exchange and correlation are included for all the metal elements in these studies. For purposes of comparisons, we performed calculations in both the *local density approximation* and the *generalized gradient approximation* to DFT for certain test cases. The LDA calculations displayed the expected overbinding relative to GGA. We performed all the interface calculations presented using the GGA. We also calculated dipole corrections perpendicular to the interface for all surface and interface structures.

The calculations consist of three stages: bulk materials calculations, surface calculations for nickel, ZrO₂, Al₂O₃, and SiO₂, and interface calculations. For the bulk calculations, we tested for convergence of the k-point sampling density and kinetic energy cutoff and relaxed the atomic and cell coordinates. We then used the most stringent k-point sampling density and kinetic energy cutoff requirements from the bulk materials calculations in the surface and interface calculations.

To aid in computational efficiency, we initially relaxed the ionic coordinates in the surface and interface structures with a 40 percent lower kinetic energy cutoff for the plane-wave basis. Once we obtained the optimized ionic coordinates with this smaller basis, we further relaxed them using the converged plane-wave basis. This allows faster structure convergence, and several test cases have shown that this does not affect the final geometries.⁵ For surface calculations, the energies are converged with respect to slab and vacuum thickness and atomic relaxations. For interface calculations, we match ideal, low-index stable surfaces of the two materials choosing an interface cell such that the lattice misfit between the materials is always under 5 percent and is generally between 1 and 3 percent in these simulations.

For several test cases, we performed high-temperature (1200 to 1600 K) molecular dynamics using Nose's algorithm for constant temperature DFT-MD, for short times (0.1 to 1.4 picoseconds using 0.4 femtosecond time steps). This annealing was designed to let the system overcome an energetically unfavorable starting configuration to reach a more favorable minimum energy structure and to test whether the relaxed structures were trapped in local minima. The interface structures

are quenched to their respective minimum energy structures from the ionic coordinates obtained at the end of the annealing run. We performed the quenching and ionic relaxations using a conjugate-gradient algorithm. The interface adhesion is defined as the energy lowering due to interface formation between the coating and the substrate, relative to the two isolated slabs, normalized by the interface surface area—that is,

$$W_{adhesion} = \frac{E_A + E_B - E_{A+B}}{Area},$$

where *A* and *B* represent the two slabs. To compare the total energy of the combined system directly with the two isolated slabs, the lattice mismatch imposed on the coating in the interface calculation is maintained for the respective isolated slab calculations. The ions are then allowed to relax subject to this constraint. By selectively varying the chemical composition at the metal slab interface, we compare the relative adhesion and bonding of several possible additions to the bond coat alloy. The alloy doping presented later is achieved by inserting half of a monolayer of the doping element between the nickel and ceramic slabs at the interface. Although we chose the initial location of these elements to fill half of the face centered cubic hollow sites on the nickel surface, the atoms are free to relax to more favorable coordinates during the simulation.

HPC resources are essential to this study. The memory requirement for the most accurate of these calculations even exploits the CPU node limits for high-performance supercomputers. We have noted a scaling efficiency of roughly 90 percent for up to 64 processors and 80 percent for 128 processors. This favorable scaling allows large-scale simulations that would be prohibitively slow on workstations or smaller parallel systems. Especially in the case of dynamics runs, an uninterrupted dedication of multiple processors lets us simulate high-temperature dynamics for timescales of physical interest. Without HPC, we would be severely restricted on feasible system size, complexity, and variety. Furthermore, we would be unable to investigate any high-temperature effects for some of the larger heterogeneous interface simulations. The importance of HPC to this work cannot be overemphasized because the extreme turbine temperatures and the metal/ceramic interface complexity in terms of chemical dopant additions are crucial aspects affecting this research's practical implications.

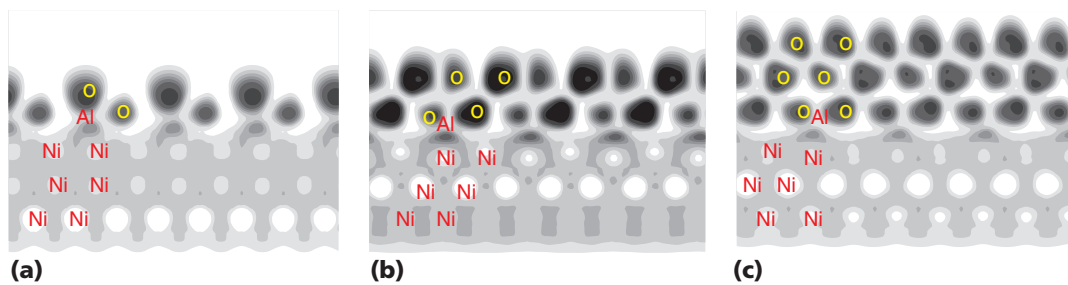


Figure 2. Electron localization function values (of the ultrasoft pseudocharge density) cut near interfacial aluminum of one, two, and three layers of Al_2O_3 on nickel. The darkest regions are the regions of highest localization.

Ideal interfaces in TBCs

Increased spallation often results from the TGO thickening with repeated thermal cycling. The TGO Al_2O_3 layer is beneficial in serving as a slow-growing, protective oxide; but the alumina layer and its interfaces with both the zirconia topcoat and the bond coat alloy are the primary locations where fracture occurs. In particular, de-adhesion at the interface with the bond coat alloy can result in the buckling and cracking that lead to spallation. Strain, introduced as a result of lattice and thermal expansion mismatch, is the favored explanation for the observed fracture and void formation in the alumina layer and at the interface with the bond coat. Although it is likely that this macroscopic strain plays a significant role in TBC failure, our studies are designed to investigate possible microscopic failure mechanisms involved in TBC spallation.

Table 1 displays the GGA calculated interfacial adhesion for the ideal interfaces of an alumina substrate with increasing zirconia film thickness and a nickel substrate with increasing ceramic, zirconia and alumina, film thicknesses.⁵⁻⁷ These interfaces represent first-order approximations of the ideal topcoat/TGO, topcoat/bond coat, and TGO/bond coat interfaces in a TBC.

The values presented in Table 1 are the interface adhesions found for our best estimates to the global minimum energy structures. As a point of

reference for these adhesion values, the calculated DFT-GGA ideal cleavage energy at 0 K of Ni(111) is approximately $3,800 \text{ mJ/m}^2$, of Al_2O_3 (0001) is roughly $3,000 \text{ mJ/m}^2$, and of ZrO_2 (111) is about $2,500 \text{ mJ/m}^2$.^{5,8} Although the adhesion at the $\text{ZrO}_2/\text{Al}_2\text{O}_3$ interface is roughly constant for increasing zirconia thickness, the adhesion value is far below the ideal cleavage energies for alumina or zirconia and is considered fairly weak for ceramic/ceramic systems. The ceramic/metal values in Table 1 are very weak, indicating that the ideal ceramic/metal interfaces of a nickel substrate with a ZrO_2 or an Al_2O_3 film coating are unfavorable. The ideal cleavage energies for any of the three bulk materials are much higher than the interface adhesion energies; as a result, it is likely TBC failure will occur at these interfaces. In particular, the metal/ceramic interface adhesion dramatically decreases for the thickest oxide films. This feature presents an atomic-level explanation for the observed spallation with increasing oxide thickness; namely, thicker oxide films prefer intracermic bonding to strong interface formation. This trend is most dramatic in the $\text{Al}_2\text{O}_3/\text{Ni}$ interface case and is an important contributor to the de-adhesion problem at that site.

In the case of $\text{Al}_2\text{O}_3/\text{Ni}$, the interface adhesion trends can be explained largely by the strength of nickel–aluminum interactions. The Al_2O_3

Table 1. Comparison of adhesion at ideal interfaces with increasing ceramic thickness. Units are energy (millijoules) per unit area (square meters).

Substrate + coating	One layer coating mJ/m^2	Two layer coating mJ/m^2	Three layer coating mJ/m^2
$\text{Al}_2\text{O}_3 + \text{ZrO}_2$	1,142	1,256	1,189
$\text{Ni} + \text{ZrO}_2$	2,011	1,308	995
$\text{Ni} + \text{Al}_2\text{O}_3$	618	943	456

Table 2. Comparison of adhesion at the ceramic/metal interface with half-monolayer element doping. Units are energy (millijoules) per unit area (square meters).

Interface Adhesion (mJ/m ²) at doped ceramic/metal interface							
	Nickel	Aluminum	Silicon	Scandium	Yttrium	Titanium	Zirconium
Ni/ZrO ₂	1,334	1,106	770	1,478	1,442	1,738	1,942
Ni/Al ₂ O ₃	1,882	1,493	1,244	3,351	3,242	3,685	3,213

monolayer rearranges such that nickel–aluminum bonds are difficult to form, and the trilayer Al₂O₃ favors aluminum–oxygen interactions instead of nickel–aluminum. Figure 2 shows a representation of this behavior, based on valence electron density analysis. The figure displays the electron localization function⁹ values on a 2D “slice” through the electron density perpendicular to the interface. The dark region between the nickel and aluminum indicates localized bond formation at this site and is most dominant for the bilayer Al₂O₃ on nickel. It can be seen that the interface adhesion values correlate with the degree of localization of the nickel–aluminum bonds formed at the interface (see Table 1). Interfacial charge transfer is negligible in all cases, and localized bonding is not observed between nickel and oxygen.

Our relative interface adhesion values suggest that spallation should occur first at the Al₂O₃/nickel interface. Although having such a prediction is useful, it is also valuable to ascertain why the interfacial adhesion exhibits these trends. Some insight into the crucial difference between alumina and zirconia lies in the bulk electronic structure of these oxides. Examination of atom-resolved densities of states indicates that whereas alumina is a very ionic oxide, zirconia is different. ZrO₂ has partially occupied *d*-states, suggesting that a fully ionic picture is incorrect and that the true oxidation state of Zr ions in zirconia is closer to Zr (II). From this, we immediately conclude then that the oxygen ions are more like O⁻ than O²⁻ in zirconia.

The implications from this bulk analysis are severe: alumina has closed-shell-like ions that cannot be expected to form strong bonds to anything, whereas zirconia has more radical (unpaired electron) character on the oxygen atoms that can form stronger bonds to late transition metal substrates. It is ironic that alumina turns out to be the main culprit in TBC spallation, because it serves the valuable function of acting as a barrier to corrosion of the nickel alloy due to alumina’s low oxygen mobility. The local bond-

ing character at the interface led us to investigate elements with open *d*-shells that could be added to the bond coat alloy to promote stronger interactions at the interface.

Improving TBC performance through reactive element additions

Our aim is to suggest chemical modifications to the bond coat that will improve adhesion at the metal/ceramic interface and inhibit oxide formation—or form oxide products more ideally suited to the imposed interface and thermal cycling requirements. Finding chemical means by which to enhance the bond coat’s ability to perform its essential roles in the TBC is no trivial matter in light of the formidable temperature cycling range and oxidative and corrosive environment of the jet engine combustion chamber. Our results indicate that doping the bond coat metal alloy with early transition metals might increase chemical bonding across the interface and result in improved adhesion. This bond coat alloy doping results in a 45 percent increased adhesion, relative to nickel, at the ZrO₂/nickel interface and a dramatic 100 percent increase in adhesion at the Al₂O₃/nickel interface.

Table 2 displays the interface adhesion values at the doped ceramic/metal interfaces. The Al₂O₃ interface doped with nickel is stronger than the ideal Al₂O₃/nickel interface presented in the previous section. This is due to the half-monolayer roughness of the nickel surface—it is less stable as an isolated slab and more inclined to form bonds at the interface due to the surface nickel atoms’ undercoordination. The series in Table 2 is presented on equal footing; the isolated and combined systems were created similarly and permitted to relax from their starting atomic configurations. Although the precise values of adhesion shown here are certainly affected by the imposed constraints, including stoichiometry, limited system size, and so on, they provide a valuable basis for relative comparison of these doping elements’ behavior in similar interfacial environments.

Formation of an alternative protective oxide layer

Although improved adhesion at the ceramic/metal and ceramic/ceramic interfaces with Al_2O_3 should aid in extending the operating lifetimes of TBCs, ideally it might prove preferable to limit or eliminate the aluminum oxide product altogether. Such a radical alteration from current bond coating materials technology requires an alternative slow-growing, protective oxide with improved adhesion properties. It is unlikely that the early transition metals could serve effectively in this capacity because they generally do not form protective oxides under the conditions present in jet engine operations. The lack of interfacial bonding resulting from the highly ionic Al_2O_3 closed-shell repulsion with the nearly filled nickel valency indicates that a more covalent oxide product might exhibit improved

Table 3. Adhesion (mJ/m^2) at the ideal SiO_2 /nickel interface with increasing SiO_2 thickness.

SiO_2 thickness (\AA)	5	10	15
W_{ad}	1,292	1,374	1,342

interface adhesion through increased chemical bonding.

Percent ionic character is not a well-defined property; nevertheless, SiO_2 is a more covalent oxide than Al_2O_3 . Silica also might be capable of forming a high-temperature protective oxide. Accordingly, we are investigating the interface between SiO_2 and nickel. Our results thus far show increased interface adhesion relative to $\text{Al}_2\text{O}_3/\text{Ni}$. For thicker films, the adhesion is more than twice as strong for silica compared to alumina. Importantly, the SiO_2/Ni interface adhesion values (see Table 3) do not exhibit the

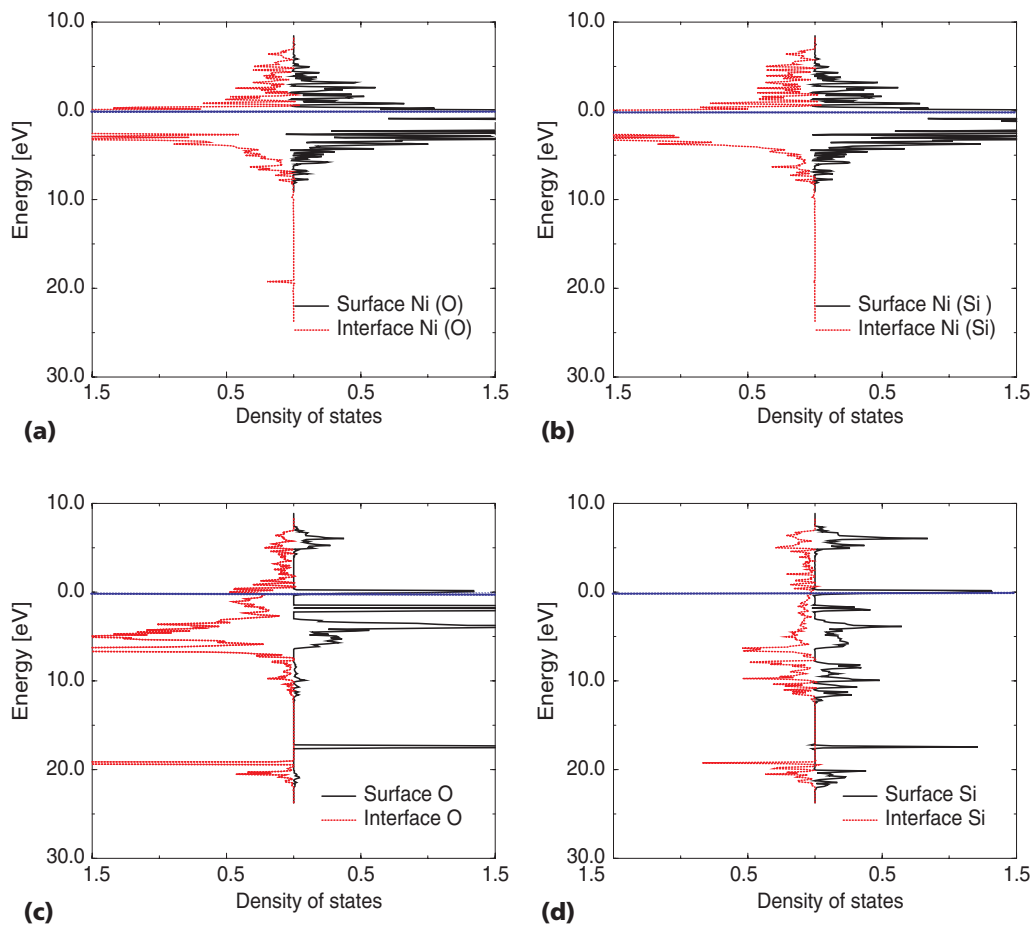


Figure 3. Projected local density of states for ions in the interface environment and the corresponding free surface environment for (a) nickel closest to oxygen at the interface, (b) nickel closest to silicon at the interface, (c) corresponding oxygen at the interface, and (d) corresponding silicon at the interface. The blue line indicates the Fermi level at 0.0 eV.

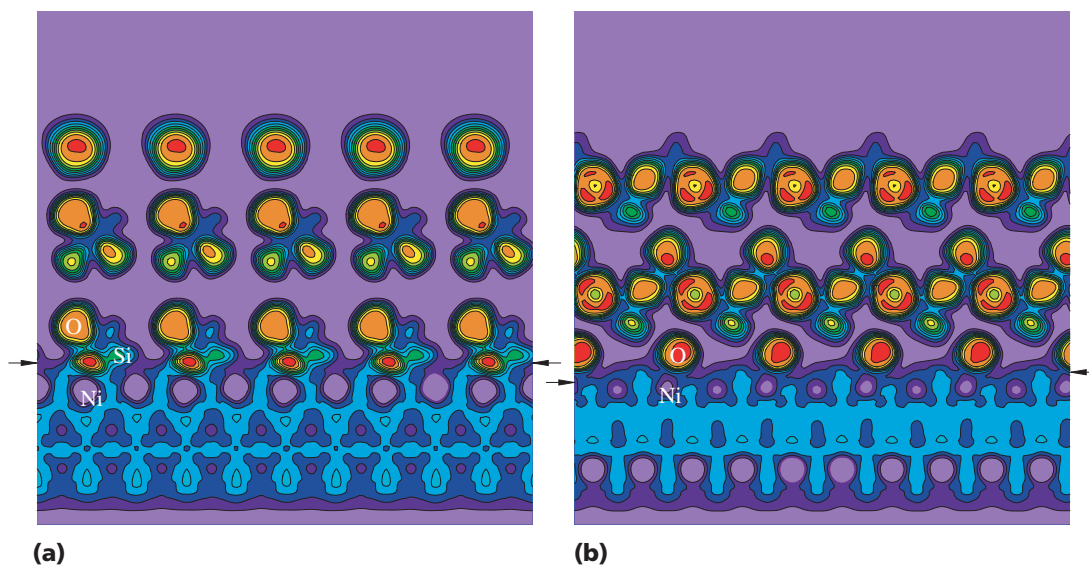


Figure 4. Electron localization function values (of the ultrasoft pseudocharge density) cut near interfacial (a) silicon and (b) oxygen of the SiO_2 /nickel interface. The black arrows indicate (a) the region of localized bonding between silicon and nickel, and (b) the lack of such a “covalent” bonding region between oxygen and nickel. The color scale runs from violet to red, with red regions representing highest electron localization.

trend of decreasing adhesion with increasing oxide thickness, as occurred with both Al_2O_3 and ZrO_2 on nickel.

Analysis of interface bonding shows that both covalent and ionic bonding play a role in the relatively strong interface adhesion. Figure 3 displays the projected local density of states for selected ions at the interface and corresponding ions in a free surface. The most dramatic difference appears in the two lower plots, with the energy decrease of the low-lying s states and removal of the dangling surface states near the Fermi level for oxygen and silicon in the interface environment. The oxygen is somewhat reduced (approximately 0.25 e⁻) in the interface environment relative to the isolated surface. Although interfacial silicon reduction is less dramatic, only roughly 0.085 e⁻, Figure 4 shows a stronger covalent-type interaction occurring between silicon–nickel than oxygen–nickel, as expected. The less ionic nature of the SiO_2 relative to Al_2O_3 allows both silicon and oxygen to participate in local bonding across the interface, leading to improved interface strength that is not affected by the increasing oxide stability that occurs during film thickening.

Although we have explored means of improving adhesion at the bond coat/ Al_2O_3 interface with early transition metal doping, it might be difficult to optimize the Al_2O_3 /YSZ interface for TBC applications. A fundamental weakness of

interfaces formed with Al_2O_3 is due to the high ionicity, and thus closed-shell-like O^{2-} behavior, in this ceramic. The SiO_2 /Ni interface is more covalently bonded and does not exhibit the unfavorable nickel–oxygen interactions displayed in the more ionic oxides. We are exploring the interface between SiO_2 and ZrO_2 ; preliminary results indicate that this interface adhesion is much stronger than that of Al_2O_3 / ZrO_2 . If these preliminary results hold true, using a silica-forming bond coat might provide an alternative intermediate layer coating that limits the spallation problem plaguing alumina-forming bond coats.

First principles calculations hold direct implications for chemically improving the performance of TBCs in jet engine turbines. The general principles that can be extracted from the trends in our analysis of a variety of ceramic and metal systems provide insight into an area of scientific interest that remains somewhat of a mystery: namely, a detailed description of the fundamental atomic-level interactions anticipated at heterogeneous interfaces. This research is intended to contribute not only to the physical understanding of these complex systems but also to technological advancements, thereby leading to performance improve-

ments of high value to both the aerospace and the electric power generation industry, which uses similar turbine technology. As a direct result of this research, we might be one step closer to more capable aircraft and more fuel-efficient power plants, with higher-performance engines capable of longer operating cycles with less maintenance and lower energy costs. 

Acknowledgments

Special thanks to the Air Force Office of Scientific Research for personnel funding. This research, in part conducted at the Maui High Performance Computing Center, was sponsored in part by the Air Force Research Laboratory, Air Force Materiel Command, USAF, under cooperative agreement number F29601-93-2-0001.

References

1. A. Christensen, E.A.A. Jarvis, and E.A. Carter, "Atomic-Level Properties of Thermal Barrier Coatings: Characterization of Metal-Ceramic Interfaces," *Chemical Dynamics in Extreme Environments, Advanced Series in Physical Chemistry*, World Scientific, Singapore, 2001, pp. 490–546.
2. H.M. Tawancy, "High-Temperature Oxidation Behavior of a Wrought Ni-Cr-W-Mn-Si-La Alloy," *Oxidation of Metals*, vol. 45, nos. 3–4, Apr. 1996, pp. 323–348.
3. D.J. Baxter et al., "The Oxidative and Corrosive Degradation of Vacuum Plasma Sprayed Coatings in Industrial Gas Turbine Environments," *Materials Science Forum*, vols. 251–254, part 2, 1997, pp. 801–808.
4. G. Kresse and J. Furthmuller, "Efficiency of Ab-initio Total Energy Calculations for Metals and Semiconductors Using a Plane-Wave Basis Set," *Computational Materials Science*, vol. 6, no. 1, July 1996, pp. 15–50.
5. E.A.A. Jarvis, A. Christensen, and E.A. Carter, "Weak Bonding of Alumina Coatings on Ni(111)," *Surface Science*, vol. 487, nos. 1–3, July 2001, pp. 55–76.
6. A. Christensen and E.A. Carter, "Adhesion of Ultrathin ZrO₂ (111) Films on Ni (111) from First Principles," *J. Chemical Physics*, vol. 114, no. 13, Apr. 2001, pp. 5816–31.
7. A. Christensen and E.A. Carter, "First Principle Characterization of a Heteroceramic Interface: ZrO₂ (001) Deposited on α -Al₂O₃ (1T02) Substrate," *Physics Review B*, vol. 62, no. 24, Dec. 2000, pp. 16,968–16,983.
8. A. Christensen and E.A. Carter, "First Principles Study of the Surfaces of Zirconia," *Physical Review B*, vol. 58, no. 12, Sept. 1998, pp. 8050–8064.
9. A.D. Becke and K.E. Edgecombe, "A Simple Measure of Electron Localization in Atomic and Molecular Systems," *J. Chemical Physics*, vol. 92, no. 9, May 1990, pp. 5397–5403.

Emily A. Carter is a professor of chemistry at the University of California, Los Angeles. Her research interests include bridging chemistry, solid state physics, materials science, and mechanical engineering, with her work focusing on linear scaling, orbital-free density functional methods that afford treatment of thousands of atoms from first principles and her embedding theory that combines quantum chemistry with periodic DFT

calculations. These techniques are now being combined with finite element approaches to undertake multi-length-scale simulations of materials. She received her BS in Chemistry at UC Berkeley and PhD in Chemistry at Caltech. Contact her at the University of California, Los Angeles, Dept. of Chemistry and Biochemistry, Box 951569, Los Angeles, CA 90095-1569; www.chem.ucla.edu/carter; eac@chem.ucla.edu.

Emily A. Jarvis is a graduate student at UCLA. Her research interests include density functional characterization of crystalline materials, surfaces, and heterogeneous interfaces. She has received a Materials Research Society Gold Award, a Ralph H. Bauer Research Award, a University of California Teaching Award, and a University of California Dissertation Year Fellowship. She received a BS in chemistry at Pepperdine University. Contact her at the University of California, Los Angeles, Dept. of Chemistry and Biochemistry, Box 951569, Los Angeles, CA 90095-1569; asche@chem.ucla.edu.

For more information on this or any other computing topic, please visit our Digital Library at <http://computer.org/publications/dlib>.

COMPUTING IN SCIENCE & ENGINEERING

**Whether You're Looking
to Hire or Be Hired,
CiSE Is Your Link to
Computing Jobs Online.**



Visit <http://computer.org/ciseportal> to job hunt right from your desktop or to hire the tops in high tech today.